International Journal of Multidisciplinary and Current Research ISSN: 2321-3124
Research Article Available at: http://ijmcr.com

Design of O-Ring with Un-Restrained Arrangement

S M Muzakkir

Department of Mechanical Engineering, Jamia Millia Islamia, New Delhi, India

Received 07 July 2022, Accepted 06 Aug 2022, Available online 09 Aug 2022, **Vol.10 (July/Aug 2022 issue)**

Abstract

The O-rings are the very commonly employed solution for creating sealing to prevent the loss of pressurized fluid or gases. In the present work the design of an O-ring with un-restrained arrangement is presented.

Keywords: *Lubricated O-ring, Un-lubricated O-ring, Sealing, Design, Leakage, Elastomers*

1. Design of Unrestrained O-ring

The unrestrained installation of the O-ring in the groove assembly pertains to the configuration when the O-ring is not in contact with the groove walls. This condition can be further classified into three different categories based upon the loading of the O-ring and the geometry of the groove into: (i) Axial O-ring, (ii) Radial Male O-ring and (iii) Radial Female O-ring. Two conditions arise when the O-ring is installed within the groove such as: (a) Unlubricated Condition and (b) Lubricated Condition, depending on whether lubrication will be provided to the O-ring prior to its installation.

2. Axial O-ring

An axially loaded groove arrangement for the O-ring is shown in the figure below:

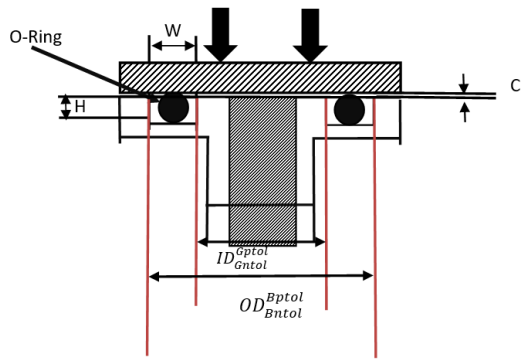

Fig. 1 Axial O-ring

The nominal inner diameter of the groove (mm) is represented by 'ID' with Gptol and Gntol representing the positive and negative tolerances on the O-ring.

Similarly, the nominal outer diameter of the groove (mm) is represented by 'OD' with the positive and negative tolerances being Bptol and Bntol respectively. The dimensions of the groove i.e. the groove width (mm) and the groove depth (mm) have been represented by 'W' and 'H' respectively while 'C' represents the separation between the sealing faces (mm). The axial O-ring is further divided into two conditions: (i) Unlubricated Condition and (ii) Lubricated Condition depending on whether lubrication will be provided to the O-ring prior to its installation in the groove assembly. Lubrication results in swelling of the O-ring resulting in an increase in the cross-sectional diameter of the O-ring.

2.1 Unlubricated condition

The unlubricated condition specifies the situation when the O-ring has been installed in the assembly without prior lubrication around the surface of the O-ring. In static applications, where movement between the sealing faces and the O-ring is negligible, unlubricated O-rings can be utilized without significantly affecting the life of the O-ring.

2.2 Cross Sectional Diameter range

The minimum diameter (d_{min}) of the O-ring is decided based on the ratio of groove width to expected minimum compression and the maximum diameter (d_{max}) decided based on the ratio of groove depth (H) to maximum compression. Above to this, the clearance and the tolerance are incorporated in estimating the diameter range of the O-ring. The (d_{min}) and (d_{max}) of the O-ring is given by equations (1) and (2) respectively. Where; '*CSptol*' is the positive tolerance on O-ring cross section (mm), *'CSntol'* is the negative tolerance on O-ring cross section (mm), 'C' is the clearance (mm), C_{min} and C_{max} is the minimum and maximum compression of the O-ring.

$$d_{min} = \frac{H}{1-C_{min}} + CSntol + C \quad (1)$$

*Corresponding author's ORCID ID: 0000-0000-0000-0000
DOI: https://doi.org/10.14741/ijmcr.v.10.4.8

$$d_{max} = \frac{H}{1 - C_{max}} + CSptol + C \quad (2)$$

2.3 Inner Diameter Range

The inner diameter of the O-ring should be greater than the nominal inner diameter of the groove for the unrestrained condition but lesser than the outer diameter of the groove. By including the tolerances of the groove, the range of inner diameter is estimated form the equation (3) and (4). Where Gntol is the negative tolerance on OD (mm) and IDN is the negative tolerance on O-ring bore (mm).

$$ID_{O-ring1} = ID_{Groove} + \left(\frac{OD-ID}{2}\right) - \frac{d}{2} - Gntol - IDN \quad (3)$$
$$ID_{O-ring2} = ID_{Groove} + \left(\frac{OD-ID}{2}\right) - \frac{d}{2} + Gptol + IDP \quad (4)$$

Where IDN and IDP represent the negative and positive tolerances on the inner diameter of the O-ring respectively.

2.4 Groove Width (GW)

The range for the groove width taking into consideration parameters such as nominal inner groove diameter, nominal outer groove diameter, the O-ring cross-section and their respective tolerances is available in the standards.

Taking into consideration the fact that if the O-ring occupies the entire groove, it will lead to the generation of increased stress which will result in shearing failure of the O-ring, in order to achieve a realistic design, the volume of the O-ring should be kept between 65-80 percent of the groove volume so that after the application of loading of the O-ring, the failure of the O-ring from extrusion can be avoided. The groove width is therefore, calculated as shown below:

$$O - ring\ volume = \frac{\pi d^2}{4} * \pi(ID + 2d) = \frac{\pi^2}{4}(ID + 2d)d^2 \quad (5)$$
$$Groove\ Volume = groovewidth * groovedepth * \pi\left(\frac{OD-ID}{2}\right) \quad (6)$$

This leads to the following two equations:

$$Groovewidth_1 = \frac{1}{0.65}\left(\frac{\pi^2 d^2 (ID+2d)}{4\left(\pi\left(\frac{OD}{2} - \frac{ID}{2}\right) * \mathrm{H}\right)}\right) - Gntol \quad (7)$$
$$Groovewidth_2 = \frac{1}{0.80}\left(\frac{\pi^2 d^2 (ID+2d)}{4\left(\left(\pi\left(\frac{OD}{2} - \frac{ID}{2}\right) * \mathrm{H}\right)\right)}\right) + Bptol \quad (8)$$

2.5 Young's Modulus (E)

Two approaches are provided for the calculation of Young's Modulus:

2.6 Using Hardness

The estimation for Young's Modulus has been formulated using the value of hardness as a parameter using the empirical relation proposed:

$$E = 0.256 * e^{0.047*(hardness - hardtol)} \quad (9)$$
$$E = 0.256 * e^{0.047*(hardness + hardtol)} \quad (10)$$

2.7 Using stress and strain values

The calculation of Young's Modulus using stress-strain values has been calculated using the Mooney-Rivlin model wherein 'f' denotes the Cauchy Stress and C_1 and C_2 are material constants.

$$f = 2\left(\frac{C_2}{\lambda} + C_1\right)\left(\lambda - \frac{1}{\lambda^2}\right) \quad (11)$$

Where '$\underline{f}$ denotes the Cauchy stress and C_2 *and* $C_1$are material constants.

2.8 Groove Height

Groove height is the sum of the groove depth value and clearance and is given by equation (12).

$$Groove\ Height = H + C \quad (12)$$

2.9 Compression in x and y direction

The O-ring though initially unrestrained, will be restrained during compression by lateral walls of the groove resulting in deformation along the surfaces of the wall. In order to account for this, the compression imposed on the O-ring needs to be normalized taking into due consideration the restraining effects of the lateral walls.

A parameter known as δ_{xy} is defined which is known as the equivalent squeeze in the x direction associated in part due to the force directly applied in the x-direction and in part due to the constraint imposed by the walls which are perpendicular to the x direction i.e. in y direction, which is shown in figure. Alternately, for restrained axial loading, δ_{yx} is the equivalent normalized squeeze on the groove walls perpendicular to the top/bottom compressive surfaces as shown.

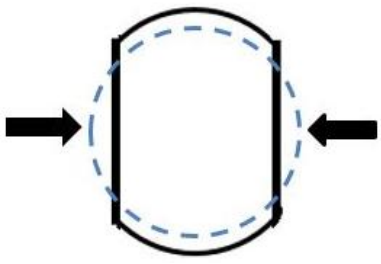

(a) δ_{xy}

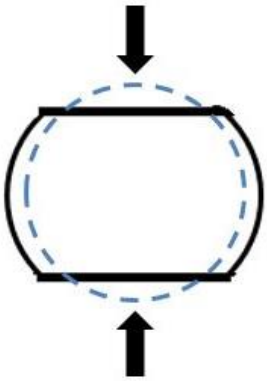

(b) δ_{yx}

Fig. 2 Compressive load applied on O-ring

By definition δ_{yx} is estimated as a ratio of difference between (i) a virtual deformed O-ring diameter along the y-axis caused by the compression (δ_{xy}); (ii) the deformed O-ring thickness, *h*. The denominator is the un-deformed O-ring diameter, '*d*'. Hence,

$$\delta_{yx} = \frac{df(\delta_{xy}) - h}{d} \Rightarrow f(\delta_{xy}) - \frac{h}{d} \quad (13)$$

Where;

$$f(\delta) = 1 + 0.415\delta_{yx} + 1.15\delta_{yx}^2 \quad (14)$$

Applying similar reasoning in the perpendicular x-direction, and using the groove width, (as the O-ring thickness), gives the equivalent squeeze

$$\delta_{xy} = \frac{df(\delta_{yx}) - GrooveWidth}{d} \Rightarrow f(\delta_{yx}) - \frac{GrooveWidth}{d} \quad (15)$$

Equations (13) and (15) are solved by iterations.

2.10 Squeeze after compressive load

The effective squeeze induced upon the O-ring is calculated from the product of deformation (δ_{xy}) and O-ring diameter (d). The formulation is given in equation (16).

$$squeeze = \delta_{yx} * d \quad (16)$$

Now, after the application of the above load, deformation takes place on the O-ring as shown below:

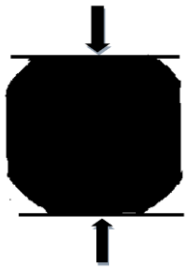

Fig. 3 O-ring deformed shape under axial loading

The deformed state of the O-ring will be analyzed using two different parameters, namely:

(A) Displacement related parameters
(B) Stress related parameters

2.11 Displacement related parameters

The compression imposed upon the O-ring will result in the generation contact width between the O-ring surface and the groove walls.

2.12 Contact width between O-ring and top (or bottom) surfaces

The contact width generated between the O-ring and the groove surface will be expressed as a product of 1.5 times the normalized compression, whose value was obtained using Eq. (13) and (15) raised to a power of (2/3).

$$Contact\ Width = 1.5 * \delta_{yx}^{2/3} \quad (17)$$

2.13 Contact width between O-ring and lateral walls

Similarly, there will be contact between the O-ring surface and the groove walls due to the restraining effects of the groove, which can be evaluated as follows:

$$Contact\ Trans = 1.5 * \delta_{xy}^{2/3} \quad (18)$$

2.14 Stress related parameters

Subsequent to deformation, our analysis proceeds to the discussion of stress related parameters. Load per unit length is estimated as a function of the Young's Modulus, cross-section diameter and the normalized compression.

$$L = E * d * \left(1.25 * \delta_{yx}^{1.5} + 50 * \delta_{yx}^{6}\right) \quad (19)$$

After evaluating the load per unit length, the total compressive force exerted by the O-ring will be the product of the load per unit length times the circumference of the O-ring i.e. (π*D).

$$Comp\_Force = \pi * L * D \quad (20)$$

The stress generated will be distributed over the contact width with its peak at the center and zero just after the edges. Therefore, we need to estimate the value of average stress exerted by the O-ring which is a function of the normalized compression times the Young's Modulus of the material.

$$Stress = E * \sqrt{\frac{8}{3\pi} * \left[1.25 * \delta_{yx}^{1.5} + 50 * \delta_{yx}^{6}\right]} \quad (21)$$

The stress generated will be distributed over the contact width with its maximum at the center of the contact width.

The stress generated will be a function of the normalized compression estimated using the least square method.

$$MaxContStress = \left(E\left(3.83\delta_{yx} - 23.00\ \delta_{yx}^2 + 82.69\ \delta_{yx}^3\right)\right) \quad (22)$$

$$MaxContStressLat = \left(E\left(2.65\delta_{xy} - 16.17\ \delta_{xy}^2 + 71.59\ \delta_{xy}^3\right)\right) \quad (23)$$

The internal fluid sealed by the O-ring will exert pressure on the O-ring, thereby, deforming it further. This consequent deformation will result in increased contact pressure generation by the O-ring. This stress is known as hydro-stress and is expressed as the product of the Poisson ratio times the fluid pressure.

$$Hydrostress = \upsilon * P_1 \quad (24)$$

Therefore, the max. stress developed by the O-ring becomes:

$$MaxContStress(MPa) = \left(E\left(3.83\delta_{xy} - 23.00\delta_{xy}^2 + 82.69\delta_{xy}^3\right)\right) + \upsilon * P_1 \quad (25)$$

$$MaxContStressLat(MPa) = \left(E\left(2.65\delta_{yx} - 16.17\delta_{yx}^2 + 71.59\delta_{yx}^3\right)\right) + \upsilon * P_1 \quad (26)$$

3 Lubricated Condition

Lubrication is provided to the O-ring in order to increase the life of the O-ring and reduce the chances of the O-ring from wearing out in any case. But the lubrication provided to the O-ring will result in the increase of the cross-section diameter of the O-ring resulting from permeation of the fluid from the O-ring material. This increased diameter is denoted by $d_1$and is dependent on sw, the percent of swell of the O-ring.

$$d_1 = d\sqrt{1 + 0.01Sw} \quad (27)$$

We proceed with the discussion of only those parameters which change as a result of the increase in the cross-sectional radius.

3.1 Normalized compression in x and y direction for lubricated O-ring

The normalized compression δ_{yx} was defined as the equivalent squeeze in the y direction associated in part due to the force directly applied in the x-direction and in part due to the constraint imposed by the walls which are perpendicular to the y direction.

$$\delta_{yx} = \frac{d_1 * f\left(\delta_{xy}\right) - h}{d_1}$$

$$\delta_{yx} = f\left(\delta_{xy}\right) - \frac{h}{d_1} \quad (28)$$

Where δ_{xy} represents the equivalent squeeze in the x-direction as a consequence of the squeeze directly applied in the x-direction and in part due to the restraining effects of the walls perpendicular to the y-direction. This is defined as:

$$\delta_{xy} = \frac{d * f\left(\delta_{yx}\right) - Groove\ Width}{d_1}$$

$$\delta_{xy} = f\left(\delta_{yx}\right) - \frac{Groove\ Width}{d_1} \quad (29)$$

The function f(δ) is defined as follows:

$$f\left(\delta_{yx}\right) = 1 + 0.415 * \delta_{yx} + 1.15 * {\delta_{yx}}^2 \quad (30)$$

Eq. (28) and (29) are solved using iterations. Represents the normalized deformed chord length of the O-ring subject to the abovementioned squeeze.

3.2 Squeeze after loading for lubricated O-ring

The normalized squeeze into the O-ring can be calculated as:

$$squeeze = \delta_{yx} * d_1 \quad (31)$$

The remaining steps involved for the case of axially loaded lubricated O-rings was similar to the case for unlubricated axially loaded O-rings,

4 Radial Male O-ring

Consider a "Radial Male O-ring" as shown in figure 4, where 'ID_{groove}' is the nominal inner diameter of the Groove (mm), '$ID_{Cylinder}$' is the nominal inner diameter of the cylinder (mm), 'W' is the groove width, 'H' is the groove depth (mm) and 'C' is the clearance between the sealing faces (mm). The positive and negative tolerance of groove inner diameter is given by Gptol and Gntol respectively. Similarly, the positive and negative tolerance of cylinder inner diameter is given by Bptol and Bntol respectively.

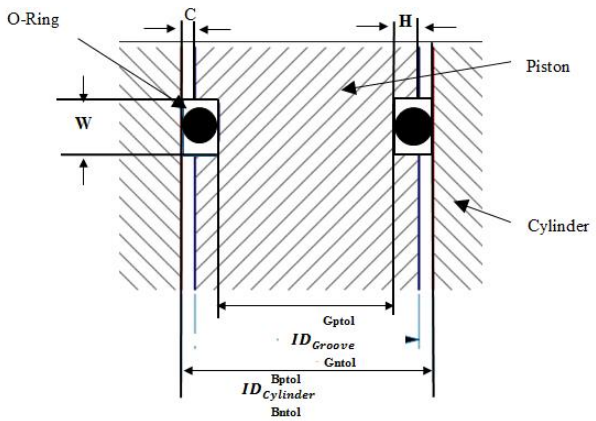

Fig. 4 Radial Male O-ring

For the Radial Male arrangement, as proposed above, two different cases are considered: (i) Unlubricated Condition and (ii) Lubricated Condition. The difference between the two arises when the O-ring is provided lubrication before its installation into the groove assembly. Since fluid permeation is an inherent property of all materials, the lubrication provided results in the swelling of the O-ring.

4.1 Unlubricated Condition

Unlubricated condition refers to the installation of the O-ring inside the assembly without prior lubrication provided to the O-ring surface. For static applications where the movement between the sealing faces and the O-ring surface is negligible, the effects of abrasion, tear, etc. are minimal and therefore, it does not drastically affect the life of the O-ring.

4.2 Cross Sectional Diameter range

The minimum diameter (d_{min}) and the maximum diameter (d_{max}) of the O-ring is decided based on the ratio of groove depth (H) to the minimum and maximum compression respectively and is calculated using Eq. (1) and (2) respectively.

4.3 Inner Diameter Range

The inner diameter of the O-ring should be greater than the nominal inner diameter of the groove for the unrestrained condition but lesser than the outer diameter of the groove. By including the tolerances of the groove, the range of inner diameter is estimated form the equation (32) and (33). Where Gntol is the negative tolerance on OD (mm) and IDN is the negative tolerance on O-ring bore (mm).

$$ID_{O-ring1} = ID_{Groove} - Gntol - IDN \quad (32)$$

$$ID_{O-ring2} = ID_{Groove} + Gptol + IDP \quad (33)$$

Where IDN and IDP represent the negative and positive tolerances on the inner diameter of the O-ring respectively.

4.4 Groove Width (GW)

The range for the groove width taking into consideration parameters such as nominal inner groove diameter, nominal inner cylinder diameter, the O-ring cross-section and their respective tolerances is available in the standards. Taking into consideration that the volume of the O-ring has been kept between 65 – 80 percent of the groove volume so as to allow for a more realistic design attainment.

$$Groovewidth_1 = \frac{1}{0.65}\left(\frac{\pi^2 d^2 (ID+2d)}{4\left(\pi\left(\frac{ID_{Cylinder}}{2} - \frac{ID_{Groove}}{2} - 2C\right)*\mathrm{H}\right)}\right) - Gntol \quad (34)$$

$$Groovewidth_2 = \frac{1}{0.80}\left(\frac{\pi^2 d^2 (ID+2d)}{4\left(\pi\left(\frac{ID_{Cylinder}}{2} - \frac{ID_{Groove}}{2} - 2C\right)*\mathrm{H}\right)}\right) + Bptol \quad (35)$$

4.5 Young's Modulus (E)

The Young's Modulus for the O-ring can be calculated using two methods: (i) Hardness and (ii) Stress-Strain values.

4.6 Groove Height

Groove height is calculated by the difference between the inner diameter of the cylinder and the groove allowing for the provision of the distance between the sealing faces and is given by equation (36).

$$Groove\ Height = ID_{Cylinder} - ID_{Groove} \quad (36)$$

4.7 Compression in x and y direction

Although the O-ring is initially unrestrained, loading upon the O-ring in the radial direction will lead to its deformation and consequently, the O-ring will come into contact with the groove walls and thereafter, stresses will generate along the surface of the groove. The compression imposed upon by radial compression, first needs to be normalized because of the axial constraining and therefore:

A parameter known as δ_{xy} which is known as the equivalent squeeze in the x direction, is defined, associated in part due to the force directly applied in the x-direction and in part due to the constraint imposed by the walls which are perpendicular to the x direction i.e. in y direction, which is shown in figure 5(a). Alternately, for restrained axial loading, δ_{yx} is the equivalent normalized squeeze on the groove walls perpendicular to the top/bottom compressive surfaces as shown in figure 5(b).

By definition δ_{yx} is estimated as a ratio of difference between (i) a virtual deformed O-ring diameter along the y-axis caused by the compression (δ_{xy}); (ii) the deformed O-ring thickness, *h*. The denominator is the un-deformed O-ring diameter, '*d*'. Hence,

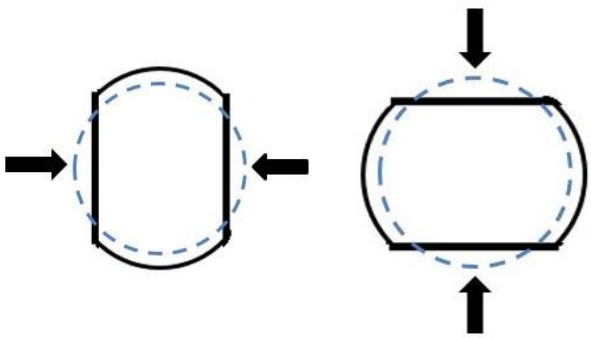

Fig. 5 Compression of O-ring

$$\delta_{xy} = \frac{df(\delta_{xy}) - H}{d} = f(\delta_{xy}) - \frac{H}{d} \quad (37)$$

Where;

$$f(\delta) = 1 + 0.415\delta_{yx} + 1.15\delta_{yx}^2 \quad (38)$$

Applying similar reasoning in the perpendicular y-direction, and using the groove width, (as the O-ring thickness), gives the equivalent squeeze

$$\delta_{yx} = \frac{df(\delta_{xy}) - GrooveWidth}{d} = f(\delta_{xy}) - \frac{GrooveWidth}{d} \quad (39)$$

Equations (37) and (39) are solved by iterations.

4.8 Squeeze

The effective squeeze induced upon the O-ring is calculated from the product of deformation (δ_{xy}) and O-ring diameter (d). The formulation is given in equation (40).

$$squeeze = \delta_{xy} * d \quad (40)$$

4.9 Contact Width

The compression imposed upon the O-ring will result in the generation of contact width between the O-ring surface and the groove walls. Hertz first evaluated the contact with generated between the O-ring surface and the groove wall but limited the case to frictionless unrestrained loading. Wendt in 1971 further extended Hertz relation by taking into consideration the effects associated with the presence of friction but restricted his calculations to the case of Unrestrained loading. In 1988, Strozzi and Dragoni examined the cases for laterally restrained O-ring seals and provided us with the following relation which has been incorporated in the software:

$$Contact\ Width = 1.5 * \delta_{xy}^{2/3} \quad (41)$$

Similarly, there will be contact between the O-ring surface and the groove walls due to the restraining effects of the groove, which can be evaluated as follows:

$$Contact\ Trans = 1.5 * \delta_{yx}^{2/3} \quad (42)$$

4.10 Contact Stress

Since the contact width was evaluated taking into consideration the effects of restraints imposed upon compression, similarly, normalized compression from equation (37) and (39) provide us the value of the load per unit length used to compress the O-ring.

$$L = E * d * \left(1.25 * \delta_{xy}^{1.5} + 50 * \delta_{xy}^{6}\right) \quad (43)$$

The total compressive force, therefore, can be calculated through:

$$Comp\_Force = \pi * L * D \quad (44)$$

The average stress acting over the O-ring was therefore:

$$Stress(MPa) = E * \sqrt{\frac{8}{3\pi} * \left[1.25 * \delta_{xy}^{1.5} + 50 * \delta_{xy}^{6}\right]} \quad (45)$$

After a series of FEM analysis carried out by Green and English, it was found out that the stress relations by Strozzi and Dragoni overestimate in values. Therefore, in order to remedy the situation, they provided empirical expressions for the peak contact stress and the peak contact lateral stress area, which are as follows:

$$MaxContStress(MPa) = \left(E\left(4.93\delta_{xy} - 32.32\ \delta_{xy}^2 + 123.63\delta_{xy}^3\right)\right) \quad (46)$$

$$MaxContStressLat(MPa) = \left(E\left(2.3\delta_{yx} - 15.35\ \delta_{yx}^2 + 76.37\ \delta_{yx}^3\right)\right) \quad (47)$$

The internal fluid sealed by the O-ring will exert pressure on the O-ring, thereby, deforming it further. This consequent deformation will result in increased contact stress generation by the O-ring. This stress is known as hydro-stress and is expressed as the ratio of the Poisson ratio divided by one minus the Poisson ratio times the fluid pressure.

$$Hydrostress = \upsilon P_1 \quad (5.48)$$

Therefore, the max. stress developed by the O-ring becomes:

$$MaxContStress(MPa) = \left(E\left(4.93\delta_{xy} - 32.32\ \delta_{xy}^2 + 123.63\delta_{xy}^3\right) + \upsilon P_1\right) \quad (49)$$

$$MaxContStressLat(MPa) = \left(E\left(2.3\delta_{yx} - 15.35\ \delta_{yx}^2 + 76.37\ \delta_{yx}^3\right) + \upsilon P_1\right) \quad (50)$$

5. Lubricated Condition

Lubrication is provided to an O-ring prior to its installation into the groove assembly, even for the case of static application of an O-ring, in order to improve the service functionality of the O-ring and helps reduce the effects of wear from creeping into the arrangement. But permeation is a property inherent to all materials, and lubrication results in the swelling of the O-ring, thereby, increasing the cross-sectional diameter of the O-ring.

If the increased cross-sectional diameter after lubrication is denoted by d_1 and the percentage of rubber swelling by sw, the new diameter can be expressed as a function of the original cross-section d and sw by the following relation:

$$d_1 = d\sqrt{1 + 0.01Sw} \quad (51)$$

This swell in diameter results in a change in a few parameters, which have been discussed in the subsequent

sections taking into consideration the increased cross-section diameter and how it affects the consequent properties.

5.1 Compression in x and y direction with lubrication

The compression taking into account the restraining effects imposed upon by the walls of the groove. With the provision of lubrication to the O-ring, the cross-sectional diameter of the O-ring changes and therefore, Eq. (37) and (39) changes and this has been shown below:

$$\delta_{xy} = \frac{d_1 f(\delta_{xy}) - H}{d_1} = f(\delta_{xy}) - \frac{H}{d_1} \quad (52)$$

$$\delta_{yx} = \frac{d_1 f(\delta_{xy}) - GrooveWidth}{d_1} = f(\delta_{xy}) - \frac{GrooveWidth}{d_1} \quad (53)$$

Equations (52) and (53) are solved by iterations.

Where d_1 represents the increased cross-sectional diameter resulting from swelling after lubrication.

5.2 Squeeze for lubricated radial O-ring

The effective squeeze induced upon the O-ring is calculated from the product of deformation (δ_{xy}) and O-ring diameter (d). The formulation is given in equation (54).

$$squeeze = \delta_{xy} * d_1 \quad (54)$$

Where d_1 represents the increased cross-sectional diameter resulting from swelling after lubrication.

5.3 Radial Female

The radial female arrangement differs from the radial male arrangement in the sense that it consists of a female groove rather than a male groove which has been cut on the outside machine part. The arrangement of a radial female O-ring is shown in figure 6 where 'OD_{piston}' is the nominal outer diameter of the piston (mm) with Gptol and Gntol as the positive and negative tolerances respectively and 'OD_{Groove}' represents the nominal outer diameter of the groove with positive and negative tolerances as Bptol and Bntol.

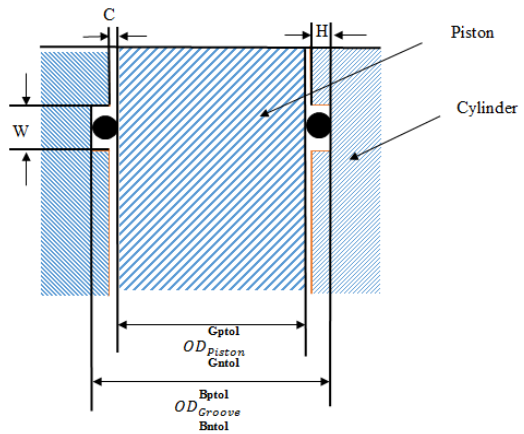

Fig. 6 Radial Female O-ring

A radial female O-ring arrangement has been shown in Fig. 6. The discussion of those parameters which change their value with the change in the geometry from a radial male arrangement to a radial female arrangement. This arrangement can be classified into two conditions: (i) Unlubricated Condition and (ii) Lubricated Condition. These two sections have been discussed below:

6. Unlubricated Condition

The condition when lubrication is not provided on the O-ring surface prior to its installation inside the assembly is known as unlubricated condition. For static applications, where movement between the sealing faces and O-ring is negligible, lubrication does not drastically affect the life of the O-ring.

6.1 Inner Diameter of the O-ring

A range for the value of the inner diameter of the O-ring taking into due consideration the unrestrained installation of the O-ring in the groove assembly, the outer diameter of the piston and the groove along with the clearance between the sealing faces along with the positive and negative tolerances of both the O-ring and the groove.

$$ID_{O-ring1} = \left(\frac{OD_{Groove} - OD_{Piston}}{2}\right) - C - Bntol - Gntol - IDN \quad (55)$$

$$ID_{O-ring2} = \left(\frac{OD_{Groove} - OD_{Piston}}{2}\right) - C - Bptol + Gptol + IDP \quad (56)$$

6.2 Groove Height for radial female O-ring

Groove height is the difference between the outer diameter of the groove and the piston which takes into consideration the clearance between the sealing faces and this is given by equation (57).

$$Groove\ Height = OD_{Groove} - OD_{Piston} \quad (57)$$

The remaining calculations of the O-ring in regards to the groove width, Young's Modulus, Compression in x and y direction, contact width and contact stress remain the same as that of radial O-ring.

6.3 Groove Width (GW)

The range for the groove width taking into consideration parameters such as nominal outer groove diameter, nominal outer piston diameter, clearance between the sealing faces, the O-ring cross-section and their respective tolerances. Taking into consideration that the volume of the O-ring has been kept between 65 – 80 percent of the groove volume so as to allow for a more realistic design attainment.

$$Groovewidth_1 = \frac{1}{0.65}\left(\frac{\pi^2 d^2 (ID+2d)}{4\left(\pi\left(\frac{OD_{Groove}}{2} - \frac{OD_{Piston}}{2} - 2C\right) * H\right)}\right) - Gntol \quad (59)$$

$$Groovewidth_2 = \frac{1}{0.80}\left(\frac{\pi^2 d^2 (ID+2d)}{4\left(\left(\pi\left(\frac{OD_{Groove}}{2} - \frac{OD_{Piston}}{2} - 2C\right) * \mathrm{H}\right)\right.}\right) - Bptol \quad (60)$$

7. Lubricated Condition

Lubrication when provided to the O-ring at the time of installation results in the increase in the cross-sectional diameter of the O-ring and thereafter, the increased diameter d_1 is calculated as a function of the initial diameter d and the percentage of swell of the O-ring 'sw'. This has been calculated in Eq. (51). The changes in the parameters of a lubricated O-ring follow the same pattern as for a radial male lubricated O-ring.

Conclusion

In the analysis for the arrangement of an unrestrained O-ring placed inside a groove arrangement three possible arrangements of the O-ring: (i) Axial, (ii) Radial Male and (iii) Radial Female has been discussed. The discussion was further sub-divided into two conditions depending on whether lubrication had been provided to the O-ring prior to its installation inside the groove assembly. The discussion began with the estimation of a few basic parameters namely groove width, groove height, cross-section diameter of the O-ring, inner diameter of the O-ring and the Young's Modulus. After the O-ring was loaded inside the groove, contact width was calculated following which the contact stress generated over the contact width was estimated. The effect of the sealed fluid pressure on the contact stress was also discussed.

References

[1] R. Flitney, *Seals and Sealing Handbook*, Sixth. Butterworth-Heinemann, 2014.

[2] P. Hannifin, *The Parker O-ring Handbook*. Pradifa.

[3] P. Kumar and H. Hirani, "Misalignment effect on gearbox failure: An experimental study," *Meas. J. Int. Meas. Confed.*, vol. 169, no. September 2020, p. 108492, 2021.

[4] K. Ghosh, S. Mazumder, B. Kumar Singh, H. Hirani, P. Roy, and N. Mandal, "Tribological Property Investigation of Self-Lubricating Molybdenum-Based Zirconia Ceramic Composite Operational at Elevated Temperature," *J. Tribol.*, vol. 142, no. 2, pp. 1–8, 2020.

[5] P. Kumar, H. Hirani, and A. Agrawal, "Fatigue failure prediction in spur gear pair using AGMA approach," *Mater. Today Proc.*, vol. 4, no. 2, pp. 2470–2477, 2017.

[6] K. P. Lijesh, D. Kumar, and H. Hirani, "Effect of disc hardness on MR brake performance," *Eng. Fail. Anal.*, vol. 74, pp. 228–238, 2017.

[7] K. P. Lijesh and H. Hirani, "Design and Development of Permanent Magneto-Hydrodynamic Hybrid Journal Bearing," *J. Tribol.*, vol. 139, no. 4, 2017.

[8] K. P. Lijesh, D. Kumar, and H. Hirani, "Synthesis and field dependent shear stress evaluation of stable MR fluid for brake application," *Ind. Lubr. Tribol.*, vol. 69, no. 5, pp. 655–665, 2017.

[9] K. P. Lijesh, D. Kumar, S. M. Muzakkir, and H. Hirani, "Thermal and frictional performance evaluation of nano lubricant with multi wall carbon nano tubes (MWCNTs) as nano-additive," *AIP Conf. Proc.*, vol. 1953, no. May, pp. 1–6, 2018.

[10] P. Kumar, H. Hirani, and A. K. Agrawal, "Online condition monitoring of misaligned meshing gears using wear debris and oil quality sensors," *Ind. Lubr. Tribol.*, vol. 70, no. 4, pp. 645–655, 2018.

[11] P. Kumar, H. Hirani, and A. Kumar Agrawal, "Effect of gear misalignment on contact area: Theoretical and experimental studies," *Measurement*, vol. 132, pp. 359–368, Jan. 2019.

[12] P. Kumar, H. Hirani, and A. Kumar Agrawal, "Effect of gear misalignment on contact area: Theoretical and experimental studies," *Meas. J. Int. Meas. Confed.*, vol. 132, pp. 359–368, 2019.

[13] P. Kumar, H. Hirani, and A. K. Agrawal, "Modeling and Simulation of Mild Wear of Spur Gear Considering Radial Misalignment," *Iran. J. Sci. Technol. - Trans. Mech. Eng.*, vol. 43, pp. 107–116, 2019.

[14] H. Hirani, T. V. V. L. N. Rao, K. Athre, and S. Biswas, "Rapid performance evaluation of journal bearings," *Tribol. Int.*, vol. 30, no. 11, pp. 825–834, 1997.

[15] H. Hirani, "Theroretical and Experimental Studies on Design of Dynamically Loaded Journal Bearing," 1998.

[16] H. Hirani, K. Athre, and S. Biswas, "Rapid and globally convergent method for dynamically loaded journal bearing design," *Proc. Inst. Mech. Eng. Part J J. Eng. Tribol.*, vol. 212, no. 3, pp. 207–213, 1998.

[17] H. Hirani, K. Athre, and S. Biswas, "Length Journal Bearings : Analytical Method of Solution," *J. Tribol.*, vol. 121, no. October, 1999.

[18] H. Hirani, K. Athre, and S. Biswas, "Dynamic analysis of engine bearings," *Int. J. Rotating Mach.*, vol. 5, no. 4, pp. 283–293, 1999.

[19] H. Hirani, K. Athre, and S. Biswas, "Comprehensive design methodology for an engine journal bearing," *Proc. Inst. Mech. Eng. Part J J. Eng. Tribol.*, vol. 214, no. 4, pp. 401–412, 2000.

[20] T. V. V. L. N. Rao, S. Biswas, H. Hirani, and K. Athre, "An analytical approach to evaluate dynamic coefficients and nonlinear transient analysis of a hydrodynamic journal bearing," *Tribol. Trans.*, vol. 43, no. 1, pp. 109–115, 2000.

[21] H. Hirani, K. Athre, and S. Biswas, "A Hybrid Solution Scheme for Performance Evaluation of Crankshaft Bearings," *J. Tribol.*, vol. 122, no. October, pp. 733–740, 2000.

[22] H. Hirani, K. Athre, and S. Biswas, "A Simplified Mass Conserving Algorithm for Journal Bearing under Large Dynamic Loads," *Int. J. Rotating Mach.*, vol. 7, no. 1, pp. 41–51, 2001.

[23] H. Hirani, K. Athre, and S. Biswas, "Lubricant shear thinning analysis of engine journal bearings," *Tribol. Trans.*, vol. 44, no. 1, pp. 125–131, 2001.

[24] R. K. Burla, P. Seshu, H. Hirani, P. R. Sajanpawar, and H. S. Suresh, "Three dimensional finite element analysis of crankshaft torsional vibrations using parametric modeling techniques," *SAE Tech. Pap.*, no. March 2020, 2003.

[25] H. Hirani and T. V. V. L. N. Rao, "Optimization of Journal Bearing Groove Geometry Using Genetic Algorithm," *NaCoMM03, IIT Delhi, India*, vol. 1, pp. 1–9, 2003.

[26] H. Hirani, "Multiobjective optimization of a journal bearing using the Pareto optimality concept," *Proc. Inst. Mech. Eng. Part J J. Eng. Tribol.*, vol. 218, no. 4, pp. 323–336, 2004.

[27] H. Hirani and P. Samanta, "Performance evaluation of magnetohydrodynamic bearing," *Proc. World Tribol. Congr. III - 2005*, pp. 97–98, 2005.

[28] H. Hirani and P. Samanta, "Test setup for magneto hydrodynamic journal bearing," in *NaCoMM-2005*, 2005, pp. 298–303.

[29] H. Hirani and N. P. Suh, "Journal bearing design using multiobjective genetic algorithm and axiomatic design approaches," *Tribol. Int.*, vol. 38, no. 5, pp. 481–491, 2005.

[30] H. Hirani, "Multiobjective optimization of journal bearing using mass conserving and genetic algorithms," *Proc. Inst. Mech. Eng. Part J J. Eng. Tribol.*, vol. 219, no. 3, pp. 235–248, 2005.

[31] P. Samanta and H. Hirani, "A simplified Optimization Approach for Permanent Magnetic Journal Bearing," *Indian J. Tribol.*, vol. 2, no. 2, pp. 23–28, 2007.

[32] H. Hirani and P. Samanta, "Hybrid (hydrodynamic + permanent magnetic) journal bearings," *Proc. Inst. Mech. Eng. Part J J. Eng. Tribol.*, vol. 221, no. 8, pp. 881–891, 2007.

[33] V. K. Sukhwani and H. Hirani, "Synthesis and characterization of low cost magnetorheological (MR) fluids," *Behav. Mech. Multifunct. Compos. Mater. 2007*, vol. 6526, p. 65262R, 2007.

[34] H. Hirani and C. S. Manjunatha, "Performance evaluation of a magnetorheological fluid variable valve," *Proc. Inst. Mech. Eng. Part D J. Automob. Eng.*, vol. 221, no. 1, pp. 83–93, 2007.

[35] P. Samanta and H. Hirani, "Magnetic Bearing Configurations: Theoretical and Experimental Studies," *IEEE Trans. Magn.*, vol. 44, no. 2, pp. 292–300, Feb. 2008.

[36] V. K. Sukhwani and H. Hirani, "Design, development, and performance evaluation of high-speed magnetorheological brakes," *Proc. Inst. Mech. Eng. Part L J. Mater. Des. Appl.*, vol. 222, no. 1, pp. 73–82, 2008.

[37] V. K. Sukhwani and H. Hirani, "A Comparative Study of Magnetorheological-Fluid-Brake and Magnetorheological-Grease-Brake," *Tribol. Online*, vol. 3, no. 1, pp. 31–35, 2008.

[38] H. Hirani and S. S. Goilkar, "Tribological Characterization of Carbon Graphite Secondary Seal," *Indian J. Tribol.*, vol. 4(2), pp. 1–6, 2009.

[39] H. Hirani and S. S. Goilkar, "Formation of transfer layer and its effect on friction and wear of carbon-graphite face seal under dry, water and steam environments," *Wear*, vol. 266, no. 11–12, pp. 1141–1154, 2009.

[40] S. S. Goilkar and H. Hirani, "Design and development of a test setup for online wear monitoring of mechanical face seals using a torque sensor," *Tribol. Trans.*, vol. 52, no. 1, pp. 47–58, 2009.

[41] H. Hirani and M. Verma, "Tribological study of elastomeric bearings for marine propeller shaft system," *Tribol. Int.*, vol. 42, no. 2, pp. 378–390, 2009.

[42] H. Hirani, "Root cause failure analysis of outer ring fracture of four-row cylindrical roller bearing," *Tribol. Trans.*, vol. 52, no. 2, pp. 180–190, 2009.

[43] H. Hirani, "Online Wear monitoring of Spur Gears," *Indian J. Tribol.*, vol. 4(2), pp. 38–43, 2009.

[44] S. S. Goilkar and H. Hirani, "Parametric study on balance ratio of mechanical face seal in steam environment," *Tribol. Int.*, vol. 43, no. 5–6, pp. 1180–1185, 2010.

[45] H. Hirani and S. S. Goilkar, "Rotordynamic Analysis of Carbon Graphite Seals of a Steam Rotary Joint," in *IuTAM Symposium on Emerging Trends in Rotor Dynamics*, 2011, pp. 253–262.

[46] S. Gupta and H. Hirani, "Optimization of magnetorheological brake," *Am. Soc. Mech. Eng. Tribol. Div. TRIB*, pp. 405–406, 2011.

[47] S. Verma, V. Kumar, and K. D. Gupta, "Performance analysis of flexible multirecess hydrostatic journal bearing operating with micropolar lubricant," *Lubr. Sci.*, vol. 24, no. 6, pp. 273–292, 2012.

[48] H. Hirani, "Online Condition Monitoring of High Speed Gears Using Vibration and Oil Anlyses," in *Thermal, Fluid and Manufacturing Sciences*, New Delhi: Narosa publishing House, 2012.

[49] C. Sarkar and H. Hirani, "Synthesis and characterization of antifriction magnetorheological fluids for brake," *Def. Sci. J.*, vol. 63, no. 4, pp. 408–412, 2013.

[50] C. Sarkar and H. Hirani, "Theoretical and experimental studies on a magnetorheological brake operating under compression plus shear mode," *Smart Mater. Struct.*, vol. 22, no. 11, 2013.

[51] C. Sarkar and H. Hirani, "Design of a squeeze film magnetorheological brake considering compression enhanced shear yield stress of magnetorheological fluid," *J. Phys. Conf. Ser.*, vol. 412, no. 1, 2013.

[52] H. Shah and H. Hirani, "Online condition monitoring of spur gears," *Int. J. Cond. Monit.*, vol. 4, no. 1, pp. 15–22, 2014.

[53] K. P. Lijesh and H. Hirani, "Magnetic bearing using rotation magnetized direction configuration," *J. Tribol.*, vol. 137, no. 4, 2015.

[54] K. P. Lijesh and H. Hirani, "Modeling and development of RMD configuration magnetic bearing," *Tribol. Ind.*, vol. 37, no. 2, pp. 225–235, 2015.

[55] C. Sarkar and H. Hirani, "Synthesis and characterization of nano-particles based magnetorheological fluids for brake," *Tribol. Online*, vol. 10, no. 4, pp. 282–294, 2015.

[56] K. P. Lijesh and H. Hirani, "Optimization of Eight Pole Radial Active Magnetic Bearing," *J. Tribol.*, vol. 137, pp. 0245021–7, 2015.

[57] P. Kumar, H. Hirani, and A. Agrawal, "Scuffing behaviour of EN31 steel under dry sliding condition using pin-on-disc machine," *Mater. Today Proc.*, vol. 2, no. 4–5, pp. 3446–3452, 2015.

[58] C. Desai, H. Hirani, and A. Chawla, "Life Estimation of Hip Joint Prosthesis," *J. Inst. Eng. Ser. C*, vol. 96, no. 3, pp. 261–267, 2015.

[59] K. P. Lijesh and H. Hirani, "Design and development of Halbach electromagnet for active magnetic bearing," *Prog. Electromagn. Res. C*, vol. 56, pp. 173–181, 2015.

[60] K. P. Lijesh and H. Hirani, "Design of Eight Pole Radial Active Magnetic Bearing using Monotonicity," in *IcIIS Conference*, 2015, no. April.

[61] K. P. Lijesh and H. Hirani, "Development of analytical equations for design and optimization of axially polarized radial passive magnetic bearing," *J. Tribol.*, vol. 137, no. 1, pp. 1–10, 2015.

[62] C. Sarkar and H. Hirani, "Development of a magnetorheological brake with a slotted disc," *Proc. Inst. Mech. Eng. Part D J. Automob. Eng.*, vol. 229, no. 14, pp. 1907–1924, 2015.

[63] C. Sarkar and H. Hirani, "Synthesis and characterisation of nano silver particle-based magnetorheological fluids for brakes," *Def. Sci. J.*, vol. 65, no. 3, pp. 252–258, 2015.

[64] C. Sarkar and H. Hirani, "Effect of Particle Size on Shear Stress of Magnetorheological Fluids," *Smart Sci.*, vol. 3, no. 2, pp. 65–73, 2015.

[65] K. P. Lijesh and H. Hirani, "Failure mode and effect analysis of active magnetic bearings," *Tribol. Ind.*, vol. 38, no. 1, pp. 90–101, 2016.

[66] C. Sarkar and H. Hirani, "Experimental studies on Magnetorheological Brake containing Plane, Holed and Slotted Discs," *Ind. Lubr. Tribol.*, vol. 69, no. 2, 2016.